



**HAL**  
open science

## Foamed Eco-Geopolymer Modified by Perlite and Cellulose as a Construction Material for Energy-Efficient Buildings

Izabela Kurek, Emilia Florek, Weronika Gozdur, Celina Ziejewska, Joanna Marczyk, Michal Łach, Kinga Korniejenko, Patrycja Duży, Marta Choińska, Magdalena Szechyńska-Hebda, et al.

► **To cite this version:**

Izabela Kurek, Emilia Florek, Weronika Gozdur, Celina Ziejewska, Joanna Marczyk, et al.. Foamed Eco-Geopolymer Modified by Perlite and Cellulose as a Construction Material for Energy-Efficient Buildings. *Energies*, 2022, 15 (12), pp.4297. 10.3390/en15124297. hal-04730895

**HAL Id: hal-04730895**

**<https://hal.science/hal-04730895v1>**

Submitted on 10 Oct 2024

**HAL** is a multi-disciplinary open access archive for the deposit and dissemination of scientific research documents, whether they are published or not. The documents may come from teaching and research institutions in France or abroad, or from public or private research centers.








L'archive ouverte pluridisciplinaire **HAL**, est destinée au dépôt et à la diffusion de documents scientifiques de niveau recherche, publiés ou non, émanant des établissements d'enseignement et de recherche français ou étrangers, des laboratoires publics ou privés.



Distributed under a Creative Commons Attribution 4.0 International License

## Article

# Foamed Eco-Geopolymer Modified by Perlite and Cellulose as a Construction Material for Energy-Efficient Buildings

Izabela Kurek <sup>1</sup>, Emilia Florek <sup>1</sup>, Weronika Gozdur <sup>1</sup>, Celina Ziejewska <sup>1</sup>, Joanna Marczyk <sup>1</sup>, Michał Łach <sup>1</sup>, Kinga Korniejenko <sup>1</sup>, Patrycja Duży <sup>2</sup>, Marta Choińska <sup>3</sup>, Magdalena Szechyńska-Hebda <sup>4,\*</sup>, and Marek Hebda <sup>1,\*</sup>

<sup>1</sup> Faculty of Materials Engineering and Physics, Cracow University of Technology, Warszawska 24, 31-155 Kraków, Poland; izabelakurek16@gmail.com (I.K.); emiflo95@gmail.com (E.F.); weronika.gozdur@gmail.com (W.G.); celina.ziejewska@gmail.com (C.Z.); jmarczyk94@gmail.com (J.M.); michal.lach@pk.edu.pl (M.Ł.); kinga.korniejenko@pk.edu.pl (K.K.)

<sup>2</sup> Faculty of Civil Engineering, Chair of Building Materials Engineering, Cracow University of Technology, 31-155 Kraków, Poland; patrycja.duzy@doktorant.pk.edu.pl

<sup>3</sup> Research Institute in Civil and Mechanical Engineering GeM, UMR CNRS 6183, Nantes University—IUT Saint-Nazaire, 44035 Nantes, France; marta.choinska@univ-nantes.fr

<sup>4</sup> Plant Breeding and Acclimatization Institute—National Research Institute, Radzików, 05-870 Błonie, Poland

\* Correspondence: szechynska@wp.pl (M.S.-H.); marek.hebda@pk.edu.pl (M.H.)

**Abstract:** Irreversible climate change, including atmosphere temperature extremes, is one of the most important issues of the present time. In this context, the construction industry requires solutions for increasing the energy efficiency of buildings through feedback between temperature adjustment inside buildings and better isolation of the external parts of buildings. Newly developed thermal insulation materials play an important role in this strategy. This paper presents the foamed geopolymer based on metakaolin that can be used as a modern facade material. In order to further improve its thermal insulation properties, the composition of geopolymer was modified with organic substances, i.e., perlite and cellulose fibers (30% and 50% of the volume). The thermal conductivity and insulation properties, density, mineral phases, absorbability, and compressive strength were improved for composite materials. It has been shown that the final properties of the foamed geopolymer can be controlled to a great extent by modifications, and the final properties determine its applicability.

**Keywords:** thermal insulation; thermal conductivity; civil engineering; compressive strength; composite materials; metakaolin



**Citation:** Kurek, I.; Florek, E.; Gozdur, W.; Ziejewska, C.; Marczyk, J.; Łach, M.; Korniejenko, K.; Duży, P.; Choińska, M.; Szechyńska-Hebda, M.; et al. Foamed Eco-Geopolymer Modified by Perlite and Cellulose as a Construction Material for Energy-Efficient Buildings. *Energies* **2022**, *15*, 4297. <https://doi.org/10.3390/en15124297>

Academic Editor: Korjenic Azra

Received: 13 May 2022

Accepted: 8 June 2022

Published: 11 June 2022

**Publisher's Note:** MDPI stays neutral with regard to jurisdictional claims in published maps and institutional affiliations.



**Copyright:** © 2022 by the authors. Licensee MDPI, Basel, Switzerland. This article is an open access article distributed under the terms and conditions of the Creative Commons Attribution (CC BY) license (<https://creativecommons.org/licenses/by/4.0/>).

## 1. Introduction

The demand for energy is increasing along with industrial development and human population growth [1,2]. According to predictions, energy consumption will increase by 53% in the next ten years [3]. In most countries, the energy use for buildings accounts for one-third of total energy consumption [4]. An energy crisis or energy shortage is a significant bottleneck in the economy. Therefore, many actions are taken to balance energy distribution, including legal regulations on the energy efficiency of residential buildings. In Europe, approximately 70% of the electric energy in the buildings is utilized for heating in winter and cooling in summer. For this reason, particular attention is now paid to the assessment and the possibility of improving the thermal performance of buildings [5]. The use of effective thermal insulation materials in residential, commercial, and industrial buildings will help reduce energy consumption, ensuring the proper urban management of energy use and smart city development. Geopolymer is a modern inorganic material intensively developed for various applications, including civil engineering. A geopolymer aluminosilicate structure is produced on the basis of various precursors, among others kaolinite, metakaolin, fly ash, or slag [6,7]. Raw materials are activated with alkaline

solutions, e.g., sodium hydroxide or potassium hydroxide mixed with sodium silicate or potassium silicate [6]. The process of hardening the geopolymer mass can take place at room temperature; however, in order to obtain better properties, heating is used at a temperature of 60 to 100 °C for 24–48 h [7]. Geopolymer is characterized by high mechanical strength, including high early compressive strength, excellent durability, good chemical resistance, and great fire resistance [6,7].

In order to achieve the great insulating properties of geopolymers, they can be produced as a porous material [8,9]. The porous structure of the geopolymer is obtained through its foaming by (1) a mechanical method, consisting of the addition of a surfactant agent, e.g., rosin, sodium dodecyl sulfate (SDS), sodium lauryl ether sulfate (SLES), Triton X-100, proteins, and mixing at a high speed; or consisting of the in situ reaction on introduced vegetable and animal fatty acids in alkali medium, known as saponification; (2) a physical method, e.g., intumescence of solid geopolymer with a higher Si/Al ratio (>20) after heating or exposition to microwave radiation; (3) a chemical method based on the chemical reactions in the presence of fine metallic powder zinc or aluminum powder that are oxidized in the presence of water and release H<sub>2</sub> gas; or H<sub>2</sub>O<sub>2</sub>, sodium hypochlorite, sodium perborate, which decompose to release O<sub>2</sub> gas; or (4) other methods, namely replica method, sacrificial filler method, and additive manufacturing [10–13].

Various additives could also be introduced into the concrete or geopolymer matrix, e.g., polypropylene fiber [14], carbon nano-tubes [15], nano-SiO<sub>2</sub> [16], and methyl 2-hydroxyethylcellulose [17], to improve thermal insulation properties. For economic and ecological reasons, additives should be cheap, commonly available, and easy to use. Organic materials such as expanded perlite or cellulose fibers meet all of these criteria.

The perlite, a siliceous amorphous volcanic rock naturally found in the environment, when rapidly heated up to 850–1000 °C can expand its original specific surface area up to 20 times. It is caused by the water molecules evaporating from the interior of the perlite [18]. The perlite, expanded in this way, has a low bulk density (0.03–0.150 g cm<sup>-3</sup>), low thermal conductivity coefficient (0.04–0.06 W m<sup>-1</sup> K<sup>-1</sup> at 24 °C), and high resistance to alkaline reaction. Therefore, expanded perlite could be used as an additive to geopolymer in order to reduce their weight and improve their insulation properties; however, only limited information on the perlite as a raw material or additive in the production of geopolymer composite can be found [19–22]. The reason for this is that perlite has long been considered an inefficient raw material that gives the final product with low mechanical properties; however, early studies applied perlite as the main alumino-silicate source [23–27]. In such case, fine perlite (e.g., d<sub>50</sub> = 6.87 μm skeletal density which is related to 2433 kg m<sup>-1</sup>) was used for geopolymer production [26]. Increasing the fineness of perlite to some extent (from 3.10 to 3.58, but not up to 4.30 m<sup>2</sup> kg<sup>-1</sup>) can improve the compressive strength amounts of the produced geopolymer and as a result its chemical resistance against aggressive agents [23]. The compressive strength of ≈30–40 MPa can be obtained [24]. The optimally fine perlite is fairly reactive, increases the compaction ratio, reduces the pores, forms a more compact structure and thus develops greater compressive strength. In contrast, a too fine fraction may cluster, and similarly, a coarse fraction acts only as a filler. The mechanical properties of geopolymers can be enhanced with increasing NaOH molarity as well as prolongation of the oven-curing period and temperatures [25]. The effect of the NaOH content during activation of the geopolymer mortar was studied within the range of 2–12 M, and the results indicated that along with its concentration increase, the setting time was longer almost six-fold. This effect did not result from changes in the solid to liquid ratio, which need to be kept constant (1.2 to 1.4 g mL<sup>-1</sup>) in order to optimize the workability of the pastes. On the other hand, the geopolymer/perlite pastes solidified faster at higher curing temperatures, with a minimum time at 100 °C [26]. The 10% addition of perlite during the synthesis of geopolymers from fly ash caused an increase in the material elasticity whilst reducing its compressive strength by 40% [28]. Waste perlite in alkaline solutions (10 M NaOH) formed crystalline zeolite 4A and other minor crystalline phases. Low compressive strength of final geopolymer material was obtained. The addition of

fly ash (41.1 wt %) or calcined kaolinic clay (10 wt %) to the perlite (22.5 wt %) improved mechanical properties to acceptable values [27,29,30]. Furthermore, compressive strength of  $\approx 50$  MPa can be obtained by partially replacing the pozzolan with 40% of the perlite, which leads to the formation of an amorphous N-A-S-H type gel. In contrast, lower compressive strength was observed along with the increase in perlite fraction, as the zeolite phase and a heterogeneous structure were developed. The maximal amount of perlite to geopolymer at which mechanical properties justify the production of the materials is 70–80% [31,32]. Perlite also reacts less effectively in a potassium-based activator [33,34].

Another useful additive of natural origin can be cellulose fibers. The good coherence between the metakaolin-based solid geopolymer matrix and cellulose fibers and good mechanical properties were found after the introduction of cellulose to geopolymer materials [35–37]. Adding fibers to the geopolymer can limit the growth of cracks, lowers density, and at the same time enhances the ductility, toughness, tensile strength, bending strength, and compressive strength of the geopolymer. However, there is a problem related to the use of natural fibers in geopolymer matrices. Natural cellulose fibers occur together with lignin, hemicellulose, and pectin [38–41], which are easily degraded in alkaline solutions to glucose and thus lower the strength of geopolymer. The content of up to 5 wt % of lignin, cellulose, and hemicellulose enhanced the flexural and compressive strength of the geopolymer. Along with the increase in cellulose fibers, the consistency of the mixture changed dramatically, becoming viscous, impairing its workability and limiting the incorporation of more cellulose [42], while fewer pores and thus a denser structure but ductile failures of final geopolymer product were observed [43]. Similarly, cellulose nanocrystals have shown considerable reinforcement potential in construction materials, provided the concentrations were less than 0.5%. The ultrasonication can disperse nanocrystals of cellulose in material, and it improves strength up to 50%, which is greater than the strength of raw cellulose (20 to 30%). The tensile strength of the geopolymer reinforced with 9% hemp fibers (vol %) was also improved to 5.5 MPa. As the content of fibers increased from 5 to 35 wt % in the geopolymer based on fly ash and sand, the mechanical properties of the final material decreased [35,44]. Geopolymer composites reinforced with 0–1 wt % maize stalk single cellulose had a sponge-like structure with 58–68% of meso and macroporosity. Measured compression strength ranged from 1 MPa up to 27 MPa [45].

The main purpose of this work was focused on the development of an eco-geopolymer with natural additives having a low thermal conductivity. The results of this study also facilitated a better understanding of the effect and behavior of cellulosic fibers and perlite in metakaolin-based geopolymers as well as the influence of reinforcement on the physical, chemical, and mechanical properties of geopolymers. Different content of additives was tested in order to design reinforced geopolymer foam as the basis for ecological applications. The developed eco-composite materials were dedicated to the thermal insulation of energy-efficient buildings and cementless material technology. Therefore, this research relates to a circular economy and zero waste approach; in addition, it responds to issues concerning a reduction in the carbon footprint and questions about global climate warming.

Geopolymer is the promising alternative to the Ordinary Portland Cement (OPC), whose annual production emits 5% to 8% of carbon dioxide responsible for global warming [46]. In contrast, four to eight times less carbon dioxide is evolved, and two to three times less energy is needed during geopolymer production [6–8]. The classification published in “the Eco-products Directory 2010” defines “eco-material” as the material with great properties, that is produced, applied, and reused, providing a minor effect on the natural environment and human population. Bearing in mind this definition, we named the materials presented here the eco-geopolymer or eco-composite material.

## 2. Materials and Methods

The basic raw material for the production of the geopolymer matrix was the metakaolin KM 60 (Keramost Company, Most, Czech Republic, Table 1). In order to improve the mechanical properties and workability, 10% of sand by weight was added to metakaolin.

Metakaolin and sand were mixed (LMB-S mixer, Geolab, Warszawa, Poland) for 10 min to the homogenous distribution of both components.

**Table 1.** The chemical composition of the metakaolin KM 60 and sand.

Oxides	Content (%)	
	Metakaolin KM 60	Sand
SiO <sub>2</sub>	50–55	90.0–90.3
Al <sub>2</sub> O <sub>3</sub>	min. 40	0.4–0.7
Fe <sub>2</sub> O <sub>3</sub>	max. 1.45	max. 0.2
CaO	0.05–0.5	0.17
MgO	0.20–0.45	0.01
K <sub>2</sub> O + Na <sub>2</sub>	max. 1.5	-
TiO <sub>2</sub>	-	0.08–0.1

An activator was made 24 h before the geopolymerization process; an aqueous solution of sodium silicate (R-145, a molar module of 2.5, ChemiKam, Będzin, Poland) was added to 8 M NaOH (Avantor Performance Materials, Gliwice, Poland) in a ratio of 2.5:1 [36]. The activator was mixed (LMB-S mixer, Geolab, Warszawa, Poland) for 1 min with raw materials at a speed of approximately 100 rpm.

A mixture of 3% hydrogen peroxide (Sigma-Aldrich) solution together with an aluminum powder (Skawina, Poland) was used as the foaming agents [47]. They were mixed (LMB-S mixer, Geolab, Warszawa, Poland) for 1 min with a mixture of raw materials and alkaline activator to produce a G type sample of geopolymer, which serves as a reference material (Table 2).

**Table 2.** Rate of raw materials, foaming agent, activators, and additives used to produce geopolymer and composites.

Sample	Sample Description	Raw Materials		Activator	Foaming Agents		Additives	
		KM 60 (% *)	Na <sub>2</sub> SiO <sub>3</sub> / NaOH (% *)	Sand (% *)	Al (% *)	H <sub>2</sub> O <sub>2</sub> (% *)	(% *)	(% **)
G	foamed geopolymer	52.5	39.3	5.8	0.6	1.8	-	-
GP30	foamed geopolymer with 30% of expanded perlite	38.4	53.1	4.3	0.5	1.4	2.3	30
GP50	foamed geopolymer with 50% of expanded perlite	36.9	53.1	4.1	0.5	1.4	4.0	50
GC30	foamed geopolymer with 30% of cellulose fibers	37.9	53.1	4.2	0.5	1.4	2.9	30
GC50	foamed geopolymer with 50% of cellulose fibers	35.9	53.1	4.0	0.5	1.4	5.1	50

\* by weight, \*\* by volume.

In order to modify the geopolymer G, the additives were introduced. The expanded perlite (EP-150, Jawar, Glińojek, Poland) with a grain size < 1.25 mm was added as the last component of the prepared geopolymer mass in an amount of 30% (GP30) and 50% (GP50) by the volume (Table 2), while cellulose fibers (ProMC2000, ProAgro, Wołomin, Poland) with an average fiber length of 1.35 mm was added in an amount of 30% (GC30) or 50% (GP50) of the volume to raw materials (metakaolin and sand) before the alkali activation (Table 2). The additives were mixed (LMB-S mixer, Geolab, Warszawa, Poland, at a speed of approximately 100 rpm) with other components for 1 min and 10 min, in order to obtain GP and GC samples, respectively.

The prepared geopolymer pastes were molded to 50 mm × 50 mm × 50 mm cubes for the compressive strength analysis or 250 mm × 250 mm × 50 mm cubes for the thermal

conductivity analysis. The specimens were cured at 70 °C for 24 h; then, they were demolded and stored under ambient conditions.

The density measurement was performed by the geometric method and with the use of a helium pycnometer. The geometric material density ( $\rho_0$ ) was determined using an electronic caliper with a measurement accuracy  $\pm 0.01$  mm (Helikos-Preisser, Gammertingen, Germany) and a laboratory balance with an accuracy  $\pm 0.001$  g (PS 1000.X2, Radwag, Radom, Poland). The skeletal density ( $\rho$ ) was determined using a helium pycnometer (Pycnomatic ATC, Thermo Fisher Scientific, Waltham, MA, USA) and helium with a purity of 99.999%. The total porosity ( $P$ ) was calculated with the equation  $P = 1 - (\rho_0/\rho)$ .

Observation of sample morphology was made by a Motic SM2-188 stereomicroscope (Motic, Hong Kong, China). In order to evaluate the internal morphology of the structure of the materials, the Y.MU2000-D X-ray detection system (YXLON, Hudson, OH, USA) was used. For each material composition, at least 3 projections were made.

The mineralogical investigation and the Rietveld quantitative phase analysis of samples were determined using X-ray diffraction (XRD). The X-ray diffraction pattern was recorded on a PANalytical Aeris diffractometer (Malvern Panalytical B.V., Almelo, The Netherlands) with a scan range from 10° to 100° 2 $\theta$ . Cu-K $\alpha$  was the source of the radiation; step size was fixed at 0.003° (2 $\theta$ ) and a time per step at 340 s. The High Score Plus software (version: 4.8, Malvern Panalytical B.V., Almelo, The Netherlands) and the ICDD (International Center for Diffraction Data, PDF4+) crystallographic database (Newtown Square, PA, USA) were used to identify the XRD diffractograms.

The water absorption test (ASTM C1585) was carried out for the samples (250 mm  $\times$  250 mm  $\times$  50 mm) immersed in the distilled water to 1/4 of their height for 30 min, 1/2 of their height for 1 h, 3/4 of their height for 1 h, and above the height for 24 h. At each time point, the samples were weighed. Water absorption ( $n$ ) was calculated according to the formula:

$$n = \frac{m_s - m_d}{m_d} * 100\%, \quad (1)$$

where

$m_s$ —the mass of the sample in a saturated state;

$m_d$ —the mass of the sample in the dry state.

The compressive strength test was carried out on the MATEST 3000 kN device. The linear rate of force increase was 1.25 kN per second. The test for each material composition was made at least three times.

Measurement of thermal conductivity at 50 °C, 30 °C, 10 °C, and  $-10$  °C was made using the HZM 446 Lambda Smal plate apparatus (NEZTSCH, Selb, Germany). The accuracy of the temperature stabilization was  $\pm 0.2$  °C.

All tests were carried out after 28 days of sample curing. All data are the average of three to six repetitions. The standard deviation was calculated and presented.

### 3. Results and Discussion

Density values determined with the geometric method and helium pycnometer are presented in Table 3. The density of porous materials, determined by the geometric method, defines space occupied within the envelope pore space of solid material and includes any interior voids, cracks, or pores (spaces within the material are included in the total volume); thus, it is named geometric, envelope, or bulk density. In contrast, skeletal density (in some cases named the true density) is the ratio of the mass of solid material to the sum of the volumes of the solid material and closed (or blind) pores within the material. The density measured by the helium pycnometer excludes open pores in the calculation, since He cannot access closed pores. Therefore, it is not surprising that the geometric density values were much lower than the skeletal density value obtained by the pycnometric method; the result confirmed many internal closed voids, cracks, or pores. The density of expanded perlite (from 0.05 to 0.15 g cm $^{-3}$ ) is much lower compared to natural cellulose fiber (from 1.5 to 1.6 g cm $^{-3}$ ), even if cellulose density differs from plant species to species

and depended on the type of preparation [33,38]; thus, GP geopolymers showed the lowest density values, regardless of the method. It was also found that the volume of additive fractions that were introduced into the geopolymer matrix, i.e., 30% or 50%, did not change significantly the density of the samples: GP30 vs. GP50 and GC30 vs. GC50. The effect was independent of the type of additive introduced and the measurement method.

**Table 3.** The density and porosity of foamed geopolymer and composite materials. Geometric density was measured with the geometric method; skeletal density was measured by the helium pycnometer; total porosity was evaluated based on geometric and skeletal density.

Sample	Geometric Density ( $\text{g cm}^{-3}$ )	Skeletal Density ( $\text{g cm}^{-3}$ )	Total Macroporosity
G	$0.69 \pm 0.08$	$2.33 \pm 0.0004$	$0.70 \pm 3$
GP30	$0.51 \pm 0.07$	$2.19 \pm 0.0005$	$0.77 \pm 3$
GP50	$0.53 \pm 0.06$	$2.16 \pm 0.0002$	$0.75 \pm 2$
GC30	$0.79 \pm 0.07$	$2.23 \pm 0.0005$	$0.65 \pm 4$
GC50	$0.73 \pm 0.09$	$2.23 \pm 0.0006$	$0.67 \pm 4$

The geometry and morphology of the additives introduced into the foamed geopolymer matrix can be a key factor in forming the various structure of porous materials. Therefore, in order to verify the influence of spherical particles of perlite vs. fibers of cellulose on the spatial structure of foamed geopolymers, their radiographs were analyzed. The representative radiographs of geopolymer and composite materials are shown in Figure 1. Pores can be clustered into few types, and micro-, meso-, and macroporous structures can be distinguished. In the case of G, GP, and GC samples, the macropore structure was defined in the earlier studies [34]. The macropores were heterogeneous in their shape, they had different sizes, and they were randomly distributed in the entire volume of the foamed geopolymer G and composite materials with the expanded perlite and cellulose. In all samples, the majority of pores had a diameter of 0.2–4 mm, similarly as reported earlier [36].

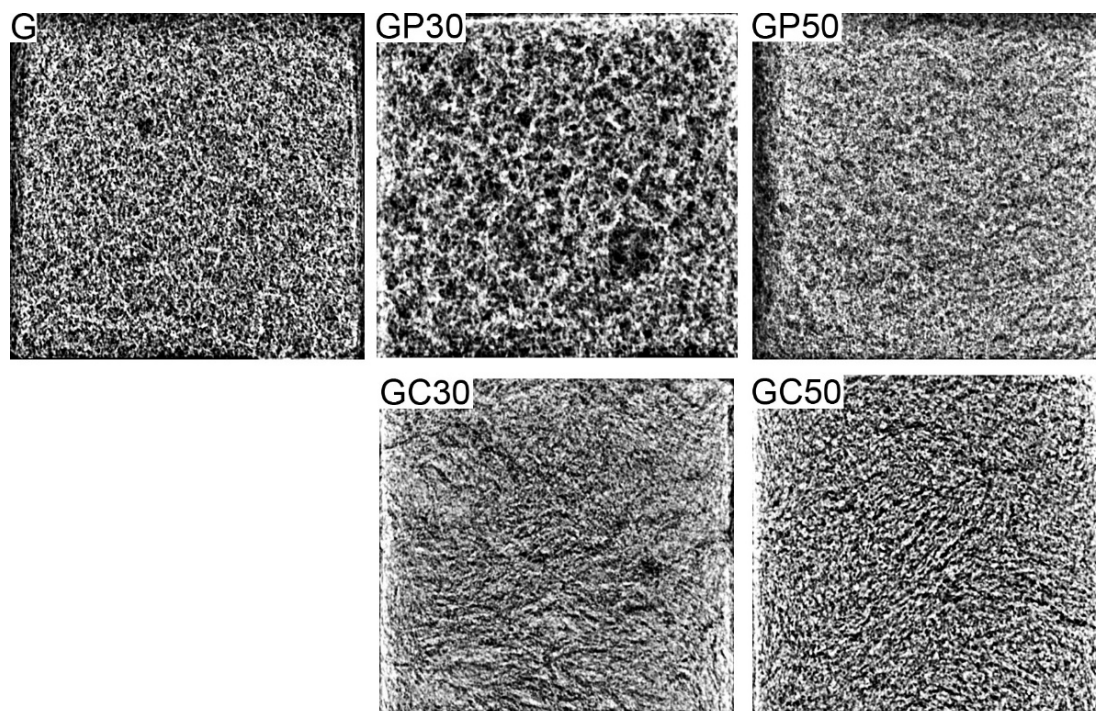


**Figure 1.** The radiographs of foamed geopolymer and composite materials with different compositions.

The decomposition/reaction of foaming agents, hydrogen peroxide and aluminum powder, respectively, produces oxygen, which produced bubbles in the geopolymer pseudo-plastic fluid paste. The pressure inside the bubbles causes their expansion and consequently geopolymer foaming. However, this effect simultaneously lowers the oxygen pressure inside the bubbles and thus reduces the foaming process [48]. Therefore, the microstructure of foam materials is dependent on the type and concentration of foaming agents as well as the composition/consistency of the paste. The sample of foamed geopolymer GP30 containing expanded perlite was characterized by a spatial structure with the different number and size of big pores. The addition of perlite beads at the last stage of the composite material production allowed the particles to retain their original shape. Thus, they could decrease the solidity of the geopolymer matrix, enable the fixing of the pores in the geopolymer matrix during the foaming process, and create additional spaces resulting from the round shape and loose packing of the perlite. A key factor of a foaming process (pore evolution and spreading) is ingredient density, which influences the viscosity of the paste [36]. An increase in the paste viscosity decreases the movement of gaseous molecules. The destabilization of bubble membranes leads to their breaking; then, they can merge, and finally, large bubbles with elongated shapes are developed (coalescence process), as observed for the GP30 sample. The density of the raw materials was  $\approx 2.6 \text{ g cm}^{-3}$  for metakaolin and  $0.05\text{--}0.15 \text{ g cm}^{-3}$  for perlite. Therefore, perlite in the geopolymer samples could reduce the viscosity of the prepared pastes and thus impair the coalescence process in the porous material. The statement was also strengthened considering the reduced geometric and skeletal density of the GP samples (Table 3). Moreover, as can be seen in Figure 1, an increase in the addition of expanded perlite from 30% to 50% reduced the foaming process, because the plastic properties of the paste decreased; thus, a network of interconnected and aggregated cells was not observed.

In contrast, cellulose fibers introduced into the geopolymer GC30 and GC50 made the spatial structure of the samples less porous compared to the G samples. The structure showed only minor discontinuities, the dimensions of which did not exceed 5 mm. The effect resulted from the elongated shape of particles, which tend to stick to each other during the preparation of geopolymer mass. The foaming agents introduced into the mixture were unable to foam geopolymer mass effectively. Additionally, the dispersion of cellulose fibers could result in their improved wettability and thus increase the consistency of the geopolymer matrix, its solidity, and homogeneity (shaping a limited number of pores and/or preventing the development of their size by the coalescence process). It was also reported earlier that geopolymer–cellulose composite foam had reduced number of the biggest pores and thus a reinforced geopolymer matrix structure [36,37]. In contrast, the geopolymer matrix of the GC organic-geopolymer hybrid foams had improved the pore number with the smallest size classes [36]. Furthermore, cellulose fibers that originated from different plants also had meso- (pore diameter of 2–50 nm) and microporous (pore diameter less than 2 nm) structures [39–41]. Bearing in mind all the above, despite having a visually more solid structure, differences in the size and number of the pores within the classes can explain the higher geometric density and at the same time lower skeletal density of GC when compared to G samples.

Apart from regular pores, in cases of both geopolymer sample types, with perlite and cellulose addition, the most important result was the lack of voids, cracks, or other internal defects visualized macroscopically, which can develop after the foaming and curing process, and in turn, greatly decrease the mechanical properties of materials.

Regardless of the composition of the foamed geopolymer and composite materials, the XRD analysis (Figure 2) showed the presence of phases rich in Si, such as quartz ( $\text{SiO}_2$ ; 01-070-2517), and phases rich in Si and Al, such as mullite ( $\text{Al}_6\text{Si}_2\text{O}_{13}$ ; 00-015-0776), kaolinite ( $\text{Al}_2\text{Si}_2\text{O}_5(\text{OH})_4$ ; 00-058-2028), and orthoclase ( $\text{KAlSi}_3\text{O}_8$ ; 00-022-1212). The main crystalline phases identified in geopolymer and composite materials were identical to those found in the raw precursor, i.e., metakaolin [49,50]. It indicated only a partial geopolymerization and the presence of unreacted particles in the geopolymers. Although the crystalline phases are



regarded as contaminants in geopolymers [51], they can positively influence the properties of final products. For instance, quartz may improve the physical and mechanical properties of final geopolymer products [52] due to the quartz particle capacity of creating barriers for crack propagation [53]. The geopolymerization process decreased the amorphous phase visible in the form of an amorphous hump in the  $2\theta$  account range between 18 and 40 when metakaolin [36,49] and geopolymer (Figure 2) were compared. The metakaolin amorphous hump had a higher intensity, while the geopolymer amorphous hump was wider and prolonged up to  $40^\circ$ . In geopolymer materials, the hump is related to glassy phases originating from quartz and mullite. The mullite and quartz phases, which do not dissolve readily in an alkaline activator, lower the effectiveness of the geopolymerization process. Furthermore, the presence of kaolinite in geopolymers may demonstrate an incomplete calcination process, which is dependent on the temperature treatment [54–56]. The crystalline structure can be broken down to form an amorphous phase during calcination at a temperature lower than that necessary to generate a liquid phase and produce glass on cooling. The orthoclase in geopolymers and composite materials contains K, which in the case of geopolymerization of the reacting minerals (dissolution and polycondensation) can have a significant effect on the increase in strength of the geopolymerization products [57,58].

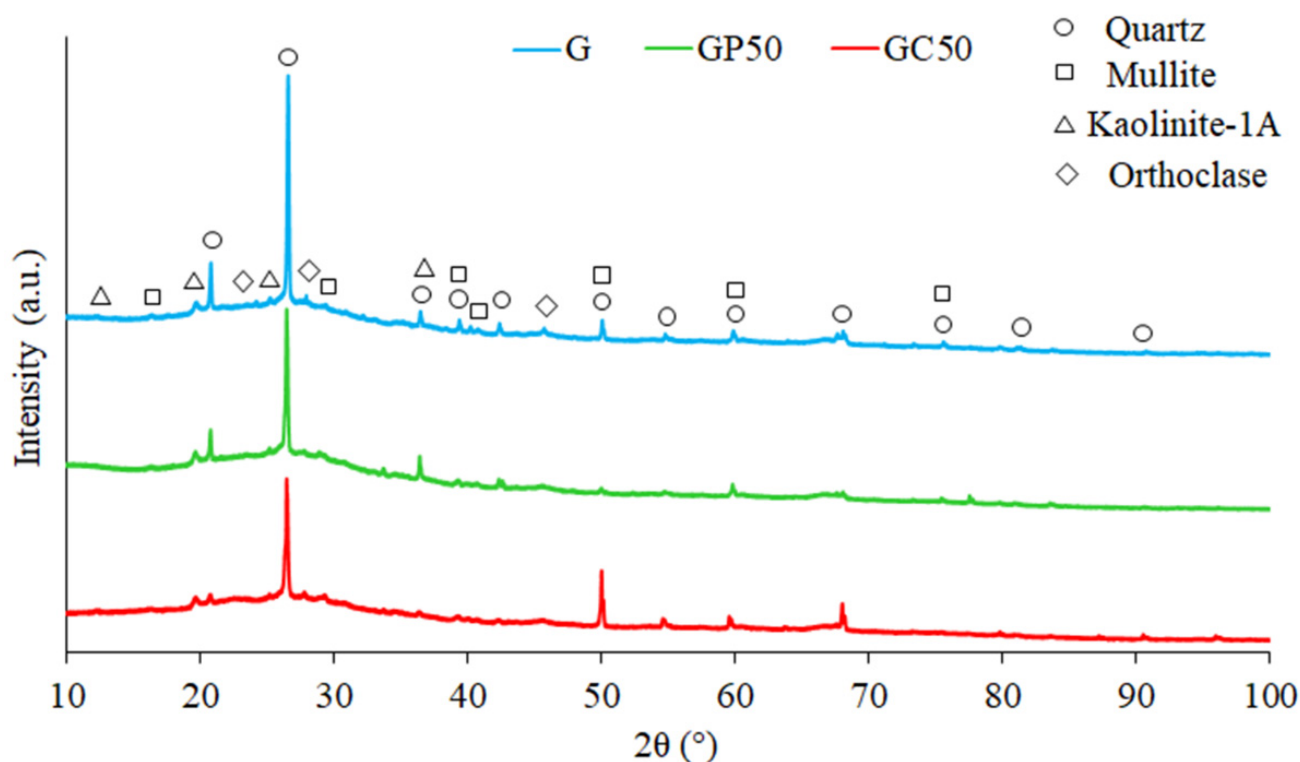


**Figure 2.** XRD patterns of foamed geopolymer and composite materials with different compositions.

The quantitative analysis of the phases in the foamed geopolymers (Table 4) showed that the addition of expanded perlite to geopolymer decreased significantly the quartz content, and to a lesser extent, the mullite content, while it increased the kaolinite and orthoclase content. The addition of cellulose fibers did not change the proportion of quartz phases compared to the G material, lowered the amount of kaolinite, and increased the mullite and orthoclase. One can conclude that the differences in geopolymer and composite materials resulted from the type of additions and the step of the protocol at which additions were incorporated. Such differences caused specific physical and mechanical properties of final materials, as described below.

**Table 4.** Quantitative analysis of foamed geopolymer and composite materials with different compositions.

		G	GP50	GC50
Phase (%)	Quartz	12.1	6.9	12.1
	Mullite	2.9	2.7	3.2
	Kaolinite-1A	17.6	19.0	10.7
	Orthoclase	67.3	71.4	74.0

The results of the absorbability test are presented in Figure 3. After a 30 min analysis, the water absorption of most of the examined foamed geopolymers was similar. The kinetics of the soaking process of the geopolymer and composite materials showed the highest values for the GP samples after 90 min. The effect was independent of the perlite volume introduced to geopolymer. The absorbability was much slower for the GC samples. The further progress of water absorption was dependent on material type; its intensity decreased over time for samples with cellulose fibers, while a continuous increase was observed for samples with expanded perlite, even after 1440 min. Finally, after 24 h, the absorbability of the samples with the addition of expanded perlite was almost 50% higher compared to the value measured for the foamed geopolymer sample. The samples containing cellulose additive achieved the water absorption values only about 10% higher compared to the G sample. The observed effects are closely related to capillary phenomena dependent on the internal structure of foamed samples (Figure 1). Porous perlite has a high water capacity and hold water in three ways: in between individual grains, on the highly irregular surfaces of each particle, and in perlite interior channels leading to the cores of the grains (Figure 1). Larger particles tend to absorb/desorb water more quickly, while the finer grades of perlite hold on the water for longer periods of time. However, crushing perlite particles during the geopolymerization process can lower the hygroscopic properties of perlite. The strong effect of crushing on the perlite permeability was also shown [59]. The cellulose has less water capacity, as the absorption area is mainly available in interior channels; thus, the effectiveness of water absorption was found to be between the G and GP samples. Although it is well known that in thermal insulation applications, porous structures are the most desirable, it should be noticed that material exposure to the water promotes the growth of microorganisms, lichens, and mosses in ambient temperatures, while the reduction in temperature can lead to the formation of cracks and degradation of the material when water is present in high amount in the interior of the material.

Although it seems that the major effect on the water absorption is the type of additive (Figure 3), it is worth noticing that the mineral composition of the geopolymer matrix can also result in lower or higher adhesive and cohesive forces interacting between the H<sub>2</sub>O and the internal surface of pores. Since the presence of kaolinite favors the more rapid water sorption/desorption, and the addition of expanded perlite to geopolymer influences the higher content of kaolinite, the improved total absorbability of GP samples can be a cumulative result of perlite and geopolymer matrix properties.

Table 5 shows the results of the compressive strength test. Geopolymer samples with the addition of expanded perlite showed about 20% lower compressive strength than G geopolymer samples. The amount of expanded perlite in the geopolymer did not have a significant impact on the compressive strength. In contrast, the addition of cellulose made the compressive strength of GC samples almost twice as high as that of the G samples. As described above, cellulose was characterized by a fibrous morphology. In GC samples, good fitting cellulose with matrix and thus restricted cracks and macropores development was observed. Together with the favorable phase composition (higher quartz and orthoclase, while lower kaolinite content in comparison to G and GP samples, Table 4), these properties resulted in the improved strength of GC samples. Interestingly, mullite rich in aluminum (Al > Si) was slightly lower in GP and higher in GC samples. Earlier, it was shown that mullite reduction can be correlated with the dealumination process. For geopolymers enriched with organic fibers GC, the mullite phase was improved and the dealumination process was inhibited; the opposite effects were observed for basic geopolymers [36,37].

The higher the mullite content and the higher the interlocking of the mullite needles, the higher the strength. The strength of the material depends on the factors that affect the amount and size of mullite needles, such as the calcination temperature and composition of alumina and silica of the raw materials.

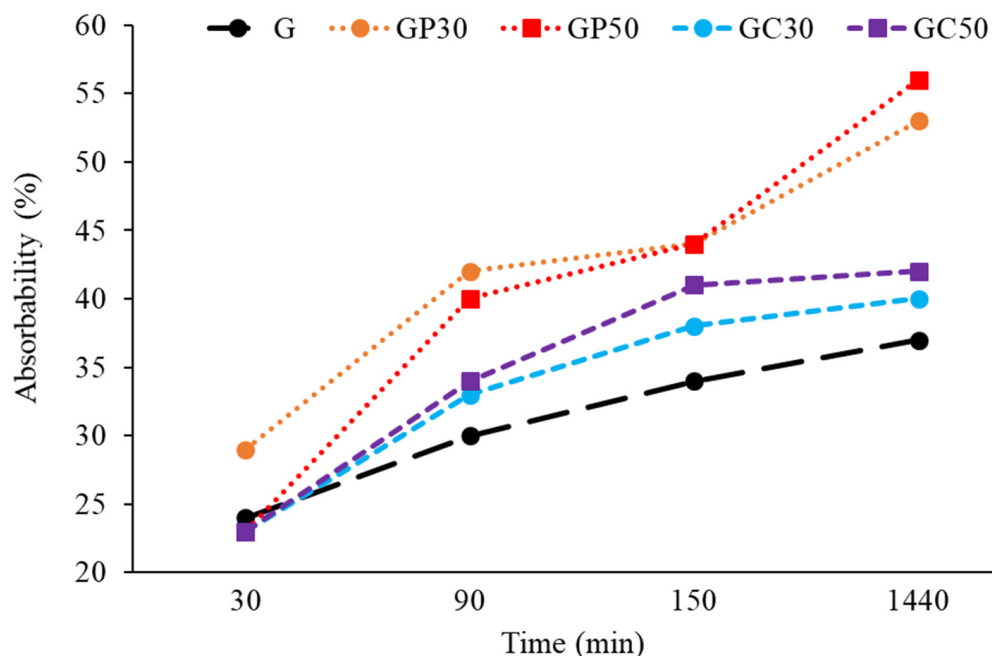


**Figure 3.** Water absorption measured after different immersion time for foamed geopolymer and composite materials with different compositions.

**Table 5.** Compressive strength of foamed geopolymer and composite materials with different compositions.

Sample	Average Compressive Strength (MPa)	Standard Deviation
G	2.32	0.26
GP30	1.87	0.52
GP50	1.82	0.30
GC30	5.47	1.2
GC50	4.27	0.7

It is well known that the thermal conductivity of a material is a measure of its ability to conduct heat, whereas thermal insulation is the thermal resistance of the unit area of a material. Heat transfer occurs at a lower rate in materials of low thermal conductivity; therefore, these are popularly used as good insulation materials. On the other hand, materials with high thermal conductivity are widely used in heat sink applications. In Table 6, the thermal properties of investigated materials are presented. It was found that regardless of the composition of the tested foamed geopolymers, with the increase in the test temperature, the value of the measured thermal conductivity increased in a linear manner, while the thermal insulation properties decreased (Figure 4). Moreover, the addition of 30% expanded perlite to the foamed geopolymer matrix caused a decrease in thermal conductivity by about 19% compared to the reference sample. This effect was repeatable regardless of the temperature at which the measurements were carried out. The increase in the volume fraction of expanded perlite from 30 to 50% resulted in a further decrease (5%) in the thermal conductivity of the tested composites. The addition of cellulose fibers also reduces the thermal conductivity of geopolymers, but this effect was not as significant as in the case of expanded perlite (8% and 18% when a 30% or 50% additive was introduced, respectively). Moreover, it was observed that depending on the measurement temperature,

the results for the same material composition differ by about 4%. This effect proves the inhomogeneity of the distribution of the additive in the structure of the produced composite and the inhomogeneity of the porosity in foamed geopolymers.

**Table 6.** Properties of concrete with porous structure according to different authors.

Material	Density ( $\text{kg m}^{-3}$ )	Compressive Strength (MPa)	Thermal Conductivity ( $\text{W m}^{-1} \text{K}^{-1}$ )	Reference
Porous concrete	–	8.0–14.7	0.47–0.87	[60]
Oil palm shell foamed concrete	1100	3.5–5.3	0.4	[61]
Cellular concrete	600	1.0–1.5	0.11–0.17	[62]
Cellular concrete	500	1.0	0.08–0.13	[62]

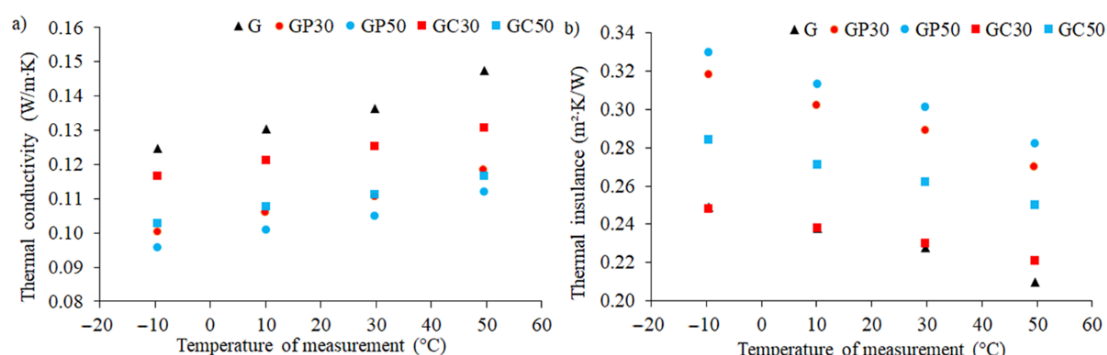


**Figure 4.** Thermal conductivity (a) and thermal insulance (b) measured at different temperatures for foamed geopolymer and composite materials with different compositions.

Rashad et al. [18] observed that the addition of expanded perlite to concrete, by partially replacing fine aggregate, resulted in increased water absorption, permeability, porosity, workability, sound insulation as well as decreased density and thermal conductivity. However, in the case of replacing cement with expanded perlite, its influence on the mechanical properties of the tested samples was ambiguous. Based on the presented results, it can be concluded that the effect of expanded perlite used as an additive to foamed geopolymers is similar to that in concrete. Table 6 shows the properties of various types of concrete with a porous structure. It can be concluded that the lower the density of these materials, the lower the compressive strength and the thermal conductivity. The analyzed foamed composite on the geopolymer matrix in terms of density can be best compared to cellular concrete with a density of  $500 \text{ kg m}^{-3}$ . Their thermal conductivity values are in the same range, but the geopolymer composite has a higher compressive strength.

Vaou and Panias [22] found that a perlite-based foamed geopolymer compared to thermal insulation materials, such as expanded and extruded polystyrene, glass, and stone wool has a thermal conductivity in the same range but a higher compressive strength, application temperature limit, and water absorption. Moreover, Papa et al. [20] examined an alkaline-bonded expanded perlite by potassium di-silicate solution. The density of the obtained material was  $467 \text{ kg m}^{-3}$ , the compressive strength was 1.6 MPa, and the thermal conductivity was  $0.084 \text{ W m}^{-1} \text{ K}^{-1}$  at  $25 \text{ }^\circ\text{C}$ . Compared to the foamed composites based on geopolymer, these materials were characterized by a similar density and compressive strength but lower thermal conductivity. In addition, Vance et al. [21] showed that perlite waste can be used as reactive aluminosilicates for the production of geopolymers and as a filler in geopolymers. This enables the use of waste materials in future research, e.g., fly ash or waste perlite instead of metakaolin and expanded perlite, which will significantly increase the ecological aspect of the produced foamed geopolymer composites.

#### 4. Conclusions

It has been shown that the geopolymer product is influenced by different variables, including properties of raw materials, i.e., the presence of specific mineralogical phases, various chemical compositions, structural, and physical properties. Further, depending on the type of the additive, the final properties of the foamed eco-geopolymer can be controlled, including its density, thermal conductivity, water absorption, and compressive strength, which can significantly affect the applicability of the products.

The use of an additive in the form of expanded perlite to the geopolymer matrix resulted in a significant decrease in thermal conductivity and density with an insignificant change in compressive strength. These composites, compared to the unmodified material, were, however, characterized by greater water absorption. This material, due to its obtained properties could be used as a thermal insulation element in construction, e.g., as a replacement for the popularly used cellular concrete. On the other hand, the use of an additive in the form of cellulose fibers increases the value of thermal conductivity compared to expanded perlite. Moreover, these composites had higher compressive strength (> 200%) when compared to the geopolymer samples without cellulose additive and lower water absorption in comparison to the composites containing the addition of expanded perlite.

Further directions of development of this type of composites are seen in the use of waste as raw materials, which will significantly increase the ecological benefits. An interest in materials dedicated to ecological buildings follows the huge environmental pressure of the global utilization of ordinary concrete. The level of demand for cement is estimated as the second-largest, just behind the level of demand for water. The development of eco-geopolymers based on waste materials with natural additives having low thermal conductivity can decrease the consumption of both energy and natural resources. For instance, the limited possibilities of the usage of class F fly ash (FFA) necessitate efforts to solve the environmental and economic problems with this waste, and FFA can serve as an excellent raw material in geopolymer with natural additives.

**Author Contributions:** Conceptualization, M.S.-H. and M.H.; Data curation, M.S.-H.; Formal analysis, E.F. and M.H.; Investigation, I.K., E.F., W.G., C.Z., J.M., M.L., K.K., P.D., M.C. and M.H.; Methodology, I.K., E.F., W.G., C.Z., J.M., M.L., K.K., P.D., M.C. and M.H.; Resources, M.H.; Supervision, M.S.-H. and M.H.; Validation, M.S.-H. and M.H.; Visualization, M.H.; Writing—original draft, I.K., E.F., W.G. and M.H.; Writing—review and editing, M.S.-H. and M.H. All authors have read and agreed to the published version of the manuscript.

**Funding:** This work has been financed by the Polish National Agency for Academic Exchange under the International Academic Partnership Program within the framework of the grant: E-mobility and sustainable materials and technologies EMMAT (PPI/APM/2018/1/00027).

**Institutional Review Board Statement:** Not applicable.

**Informed Consent Statement:** Not applicable.

**Data Availability Statement:** Not applicable.

**Acknowledgments:** The research was part of the work provided by the interdisciplinary research group Geopolymer composites for construction (GEOMAT).

**Conflicts of Interest:** The authors declare no conflict of interest. The funders had no role in the design of the study; in the collection, analyses, or interpretation of data; in the writing of the manuscript, or in the decision to publish the results.

#### References

1. Wanga, X.C.; Klemeša, J.J.; Dongb, X.; Fanb, W.; Xub, Z.; Wangc, Y.; Varbanova, P.S. Air pollution terrain nexus: A review considering energy generation and consumption. *Renew. Sustain. Energy Rev.* **2019**, *105*, 71–85. [[CrossRef](#)]
2. Wu, X.D.; Guo, J.L.; Ji, X.; Chen, G.Q. Energy use in world economy from household-consumption-based perspective. *Energy Policy* **2019**, *127*, 287–298. [[CrossRef](#)]
3. Aditya, L.; Mahlia, T.M.I.; Rismanchi, B.; Ng, H.M.; Hasan, M.H.; Metselaar, H.S.C.; Muraza, O.; Aditiya, H.B. A review on insulation materials for energy conservation in buildings. *Renew. Sustain. Energy Rev.* **2017**, *73*, 1352–1365. [[CrossRef](#)]

4. Asadi, I.; Shafiqh, P.; Hassan, Z. Thermal conductivity of concrete—A review. *J. Build. Eng.* **2018**, *20*, 81–93. [[CrossRef](#)]
5. Aydin, E.; Brounen, D. The impact of policy on residential energy consumption. *Energy* **2019**, *196*, 115–129. [[CrossRef](#)]
6. Singh, B.; Ishwarya, G.; Gupta, M.; Bhattacharyya, K. Geopolymer concrete: A review of some recent developments. *Constr. Build. Mater.* **2015**, *85*, 78–90. [[CrossRef](#)]
7. Zhang, P.; Zheng, Y.; Wang, K.; Zhang, J. A review on properties of fresh and hardened geopolymer mortar. *Compos. Part B Eng.* **2018**, *152*, 79–95. [[CrossRef](#)]
8. Dhasindrakrishna, K.; Pasupathy, K.; Ramakrishnan, S.; Sanjayan, J. Progress, current thinking and challenges in geopolymer foam concrete technology. *Cem. Concr. Compos.* **2021**, *116*, 103886. [[CrossRef](#)]
9. Ercoli, R.; Laskowska, D.; Nguyen, V.V.; Le, V.S.; Louda, P.; Łoś, P.; Ciemnicka, J.; Prałat, K.; Renzulli, A.; Paris, E.; et al. Mechanical and Thermal Properties of Geopolymer Foams (GFs) Doped with By-Products of the Secondary Aluminum Industry. *Polymers* **2022**, *14*, 703. [[CrossRef](#)]
10. Singh, N.B. Foamed geopolymers concrete. *Mater. Today: Proc.* **2018**, *5*, 15243–15252. [[CrossRef](#)]
11. Kränzlein, E.; Pöllmann, H.; Krcmar, W. Metal powders as foaming agents in fly ash based geopolymer synthesis and their impact on the structure depending on the Na/Al ratio. *Cem. Concr. Compos.* **2018**, *90*, 161–168. [[CrossRef](#)]
12. Kioupis, D. Development of porous geopolymers foamed by aluminum and zinc powders. *Ceram. Int.* **2021**, *46*, 26280–26292. [[CrossRef](#)]
13. Łach, M.; Korniejewski, K.; Miłucha, J. Thermal insulation and thermally resistant materials made of geopolymers foam. *Procedia Eng.* **2016**, *151*, 410–416. [[CrossRef](#)]
14. Awang, H.; Mydin, A.O.; Roslan, A. Effect of additives on mechanical and thermal properties of lightweight foamed concrete. *Adv. App. Sci. Res.* **2012**, *3*, 3326–3338.
15. Yakovlev, G.; Keriene, J.; Gailus, A.; Girniene, I. Cement based foam concrete reinforced by carbon nanotubes. *ISSN Mater. Sci.* **2006**, *12*, 147–151.
16. Saleh, A.N.; Attar, A.A.; Ahmed, O.K.; Mustafa, S.S. Improving the thermal insulation and mechanical properties of concrete using Nano-SiO<sub>2</sub>. *Results Eng.* **2021**, *12*, 100303. [[CrossRef](#)]
17. Prałat, K.; Jaskulski, R.; Ciemnicka, J.; Makomaski, G. Analysis of the thermal properties and structure of gypsum modified with cellulose based polymer and aerogels. *Arch. Civ. Eng.* **2020**, *66*, 153–168.
18. Rashad, A.M. A synopsis about perlite as building material—A best practice guide for Civil Engineer. *Constr. Build. Mater.* **2016**, *121*, 338–353. [[CrossRef](#)]
19. Erdoğan, S.T. Use of perlite to produce geopolymers, 31st cement and concrete science conference novel developments and innovation in cementitious materials. In Proceedings of the 31st Cement and Concrete Science Conference Paper Number XX Novel Developments and Innovation in Cementitious Materials, London, UK, 12–13 September 2011.
20. Papa, E.; Medri, V.; Murri, A.N.; Laghi, L.; De Aloysio, D.; Bandini, S.; Landi, E. Characterization of alkali bonded expanded perlite. *Constr. Build. Mater.* **2018**, *191*, 1139–1147. [[CrossRef](#)]
21. Vance, E.R.; Perera, D.S.; Imperia, P.; Cassidy, D.J.; Davis, J.; Gourley, J.T. Perlite waste as a precursor for geopolymer formation. *J. Aust. Ceram. Soc.* **2009**, *45*, 44–49.
22. Durmuş, G.; Uluer, O.; Aktaş, M.; Karaağaç, I.; Khanlari, A.; Ağbulut, U.; Çelik, D.N. A Study on Some Factors Affecting on CO<sub>2</sub> Curing of Expanded Perlite Based Thermal Insulation Panel. In *Lecture Notes in Civil Engineering, Proceedings of the 3rd International Sustainable Buildings Symposium, held in Dubai, United Arab Emirates, 15–17 March 2017*; Fratt, S., Kinuthia, J., Abu-Tair, A., Eds.; Springer: Berlin/Heidelberg, Germany, 2018. [[CrossRef](#)]
23. Mohabbi, M. Investigation of sulfates effects in perlite-based geopolymer. *Struct Concr.* **2019**, *20*, 1402–1410. [[CrossRef](#)]
24. Çelikten, S.; Işıkdag, B. Properties of geopolymer mortars derived from ground calcined perlite and NaOH solution. *Eur. J. Environ. Civil Eng.* **2021**, *26*, 1879939. [[CrossRef](#)]
25. Çelikten, S.; Işıkdag, B. Strength development of ground perlite-based geopolymer mortars. *Adv. Concr. Constr.* **2020**, *9*, 227–234. [[CrossRef](#)]
26. Tsaousi, M.; Douni, I.; Panyas, D. Characterization of the properties of perlite geopolymer pastes. *Mater. Constr.* **2016**, *66*, e102. [[CrossRef](#)]
27. Erdogan, S.T. Properties of Ground Perlite Geopolymer Mortars. *J. Mater. Civil Eng.* **2015**, *27*. [[CrossRef](#)]
28. Baran, P.; Nazarko, M.; Włosińska, E.; Kanciruk, A.; Zarebska, K. Synthesis of geopolymers derived from fly ash with an addition of perlite. *J. Clean. Prod.* **2021**, *293*, 126112. [[CrossRef](#)]
29. Aziz, A.; Benzaouak, A.; Bellil, A.; Alomayri, T.; Ni el Hassani, I.-E.E.; Achab, M.; Azhari, H.E.; Et-Tayea, Y.; Shaikh, F.U.A. Effect of acidic volcanic perlite rock on physio-mechanical properties and microstructure of natural pozzolan based geopolymers. *Case Stud. Constr. Mater.* **2021**, *15*, e00712. [[CrossRef](#)]
30. Voottipruex, P.; Teerawattanasuk, C.; Sramoon, W.; Meepon, I. Stabilization of Soft Clay Using Perlite Geopolymer Activated by Sodium Hydroxide. *Int. J. Geosynth. Ground Eng.* **2022**, *8*, 5. [[CrossRef](#)]
31. Szabó, R.; Dolgos, F.; Debreczeni, A.; Mucsi, G. Characterization of mechanically activated fly ash-based lightweight geopolymer composite prepared with ultrahigh expanded perlite content. *Ceram. Int.* **2022**, *48*, 4261–4269. [[CrossRef](#)]
32. Saufi, H.; Alouani, M.E.; Alehyen, S.; Achouri, M.E.; Aride, J.; Taibi, M. Photocatalytic Degradation of Methylene Blue from Aqueous Medium onto Perlite-Based Geopolymer. *Int. J. Chem. Eng.* **2020**, *2020*, 9498349. [[CrossRef](#)]

33. Szechyńska-Hebda, M.; Czarnocka, W.; Hebda, M.; Karpiński, S. PAD4, LSD1 and EDS1 regulate drought tolerance, plant biomass production, and cell wall properties. *Plant Cell Rep.* **2016**, *35*, 527–539. [[CrossRef](#)] [[PubMed](#)]
34. Rouquerol, J.; Avnir, D.; Fairbridge, C.W.; Everett, D.H.; Haynes, J.H.; Pernicone, N.; Ramsay, J.D.F.; Sing, K.S.W.; Unger, K.K. Recommendations for the characterization of porous solids. *Pure Appl. Chem.* **1994**, *66*, 1739–1758. [[CrossRef](#)]
35. Liu, J.; Lv, C. Durability of Cellulosic-Fiber-Reinforced Geopolymers: A Review. *Molecules* **2022**, *27*, 796. [[CrossRef](#)] [[PubMed](#)]
36. Szechyńska-Hebda, M.; Marczyk, J.; Ziejewska, C.; Hordyńska, N.; Mikuła, J.; Hebda, M. Optimal Design of pH-neutral Geopolymer Foams for Their Use in Ecological Plant Cultivation Systems. *Materials* **2019**, *12*, 2999. [[CrossRef](#)] [[PubMed](#)]
37. Szechyńska-Hebda, M.; Marczyk, J.; Ziejewska, C.; Hordyńska, N.; Mikuła, J.; Hebda, M. Neutral geopolymer foams reinforced with cellulose studied with the FT-Raman spectroscopy. In *IOP Conference Series: Materials Science and Engineering*; IOP Publishing: Bristol, UK, 2019; Volume 706, p. 012017.
38. Szechyńska-Hebda, M.; Hebda, M.; Mirek, M.; Miernik, K. Cold-induced changes in cell wall stability determine the resistance of winter triticale to fungal pathogen *Microdochium nivale*. *J. Anal. Calorim.* **2016**, *126*, 77–90. [[CrossRef](#)]
39. Szechyńska-Hebda, M.; Hebda, M.; Mierzwiński, D.; van Ammeren, A.; Karpiński, S. Effect of cold-induced changes in physical and chemical leaf properties on the resistance of winter triticale (*×Triticosecale*) to the fungal pathogen *Microdochium nivale*. *Plant Pathol.* **2013**, *62*, 867–878. [[CrossRef](#)]
40. Szechyńska-Hebda, M.; Wasek, I.; Gołbiowska, G.; Żur, I.; Wedzony, M. Photosynthesis dependent physiological and genetic crosstalk between cold acclimation and cold-induced resistance to fungal pathogens in triticale (*Triticosecale* Wittm.). *J. Plant Physiol.* **2015**, *177*, 30–43. [[CrossRef](#)]
41. Ślesak, I.; Szechyńska-Hebda, M.; Fedak, H.; Sidoruk, N.; Dąbrowska-Bronk, J.; Witoń, D.; Rusaczek, A.; Antczak, A.; Drożdżek, M.; Karpińska, B.; et al. PHYTOALEXIN DEFICIENT 4 affects reactive oxygen species metabolism, cell wall and wood properties in hybrid aspen (*Populus tremula* L.  $\times$  *tremuloides*). *Plant Cell Environ.* **2015**, *38*, 1275–1284. [[CrossRef](#)]
42. Lazorenko, G.; Kasprzhitskii, A.; Mischinenko, V.; Kruglikov, A. Fabrication and characterization of metakaolin-based geopolymer composites reinforced with cellulose nanofibrils. *Mater. Lett.* **2022**, *308*, 131146. [[CrossRef](#)]
43. Ye, H.; Zhang, Y.; Yu, Z.; Mu, J. Effects of cellulose, hemicellulose, and lignin on the morphology and mechanical properties of metakaolin-based geopolymer. *Constr. Build. Mater.* **2018**, *173*, 10–16. [[CrossRef](#)]
44. Rahmawati, C.; Aprilia, S.; Saidi, T.; Aulia, T.B. Current development of geopolymer cement with nanosilica and cellulose nanocrystals. *J. Phys. Conf. Ser.* **2021**, *1783*, 012056. [[CrossRef](#)]
45. Youmoue, M.; Tene Fongang, R.T.; Gharzouni, A.; Kaze, R.C.; Kamseu, E.; Sglavo, V.M.; Kenfack, I.T.; Nait-Ali, B.; Rossignol, S. Effect of silica and lignocellulosic additives on the formation and the distribution of meso and macropores in foam metakaolin-based geopolymer filters for dyes and wastewater filtration. *SN Appl. Sci.* **2020**, *2*, 642. [[CrossRef](#)]
46. Nguyen, V.V.; Le, V.S.; Louda, P.; Szczypiński, M.M.; Ercoli, R.; Růžek, V.; Łoś, P.; Prałat, K.; Plaskota, P.; Pacyniak, T.; et al. Low-Density Geopolymer Composites for the Construction Industry. *Polymers* **2022**, *14*, 304. [[CrossRef](#)] [[PubMed](#)]
47. Łach, M. Geopolymer Foams—Will They Ever Become a Viable Alternative to Popular Insulation Materials?—A Critical Opinion. *Materials* **2021**, *14*, 3568. [[CrossRef](#)]
48. Vaou, V.; Pnias, D. Thermal insulating foamy geopolymers from perlite. *Miner. Eng.* **2010**, *23*, 1146–1151. [[CrossRef](#)]
49. Mierzwiński, D.; Łach, M.; Hebda, M.; Walter, J.; Szechyńska-Hebda, M.; Mikuła, J. Thermal phenomena of alkali-activated metakaolin studied with a negative temperature coefficient system. *J. Therm. Anal. Calorim.* **2019**, *138*, 4167–4175. [[CrossRef](#)]
50. Marczyk, J.; Ziejewska, C.; Gądek, S.; Korniejewski, K.; Łach, M.; Góra, M.; Kurek, I.; Doğan-Sağlamtimur, N.; Hebda, M.; Szechyńska-Hebda, M. Hybrid Materials Based on Fly Ash, Metakaolin, and Cement for 3D Printing. *Materials* **2021**, *14*, 6874. [[CrossRef](#)]
51. Caballeroa, L.R.; das Dores Macedo Paivaa, M.; de Moraes Rego Fairbairna, E.; Dias Toledo Filhoa, R. Thermal, Mechanical and Microstructural Analysis of Metakaolin Based Geopolymers. *Mater. Res.* **2019**, *22*, e20180716. [[CrossRef](#)]
52. Osholana, T.S.; Dłudlu, M.K.; Oboirien, B.; Sadiku, R. Enhanced reactivity of geopolymers produced from fluidized bed combustion bottom ash. *S. Afr. J. Chem. Eng.* **2020**, *34*, 72–77. [[CrossRef](#)]
53. Ziejewska, C.; Marczyk, J.; Korniejewski, K.; Bednarz, S.; Sroczyk, P.; Łach, M.; Mikuła, J.; Figiela, B.; Szechyńska-Hebda, M.; Hebda, M. 3D Printing of Concrete-Geopolymer Hybrids. *Materials* **2022**, *15*, 2819. [[CrossRef](#)] [[PubMed](#)]
54. Łach, M.; Gado, R.A.; Marczyk, J.; Ziejewska, C.; Dogan-Saglamtimur, N.; Mikuła, J.; Szechyńska-Hebda, M.; Hebda, M. Process design for a production of sustainable materials from post-production clay. *Materials* **2021**, *14*, 953. [[CrossRef](#)] [[PubMed](#)]
55. Zenabou, N.N.M.; Benoit-Ali, N.; Zekeng, S.; Rossignol, S.; Melo, U.C.; Tchamba, A.B.; Kamseu, E.; Leonelli, C. Improving insulation in metakaolin based geopolymer: Effects of metabauxite and metatalc. *J. Build. Eng.* **2019**, *23*, 403–413. [[CrossRef](#)]
56. Kocak, Y. Effects of metakaolin on the hydration development of Portland-composite cement. *J. Build. Eng.* **2020**, *31*, 101419. [[CrossRef](#)]
57. Prasanphan, S.; Wannagon, A.; Kobayashi, T.; Jiemsirilers, S. Reaction mechanisms of calcined kaolin processing waste-based geopolymers in the presence of low alkali activator solution. *Constr. Build. Mater.* **2019**, *221*, 409–420. [[CrossRef](#)]
58. Xu, H.; van Deventer, J.S.J. The geopolymerisation of aluminosilicate minerals. *Int. J. Miner. Process.* **2000**, *59*, 247–266. [[CrossRef](#)]
59. Jamei, M.; Guiras, H.; Chtourou, Y.; Kallel, A.; Romero, E.; Georgopoulos, I. Water retention properties of perlite as a material with crushable soft particles. *Eng. Geol.* **2011**, *122*, 261–271. [[CrossRef](#)]
60. Chen, J.; Wangb, H.; Xie, P.; Najm, H. Analysis of thermal conductivity of porous concrete using laboratory measurements and microstructure models. *Constr. Build. Mater.* **2019**, *218*, 90–98. [[CrossRef](#)]

- 
61. Alengaram, U.J.; Muhit, B.A.A.; bin Jumaat, M.Z.; Liu, M.; Jing, Y. A comparison of the thermal conductivity of oil palm shell foamed concrete with conventional materials. *Mater. Des.* **2013**, *51*, 522–529. [[CrossRef](#)]
  62. Chica, L.; Alzate, A. Cellular concrete review: New trends for application in construction. *Constr. Build. Mater.* **2019**, *200*, 637–647. [[CrossRef](#)]